

Chapter 2

PID Control

The use of Proportional-Integral-Derivative (PID) controllers for integrating processes with dead time is discussed in this chapter. Since PID controllers are the most adopted controllers in industry and there are many different design methods, only those techniques specialised for IPDT processes are discussed in this chapter. After having introduced PID controllers, identification methods suitable to be applied in an industrial context are presented. Both open-loop and (relay-feedback-based) closed-loop techniques are considered. Then, tuning methods are explained. Without aiming at presenting all the tuning methods proposed in the literature, different approaches are highlighted with the purpose of showing how the problem can be tackled from different points of view. After having presented empirical tuning rules, analytical design techniques are explained, in particular those based on the Internal Model Control. Then, frequency domain approaches are discussed. Subsequently, techniques based on optimisation criteria are presented, in particular those based on the optimisation of integral criteria and on H_∞ loop shaping. Note that the classification done hereafter is subjective because, actually, there might be overlap between the different methods considered (for example, the Internal Model Control strategy is analytical, but, at the same time, it minimises integral criteria).

2.1 PID Controllers

2.1.1 Basic Principles

PID controllers are the most adopted controllers in industrial settings owing to their relative ease of use and the satisfactory performance they are capable to provide for the great majority of processes. Indeed, the cost/benefit ratio they can achieve is difficult for other kinds of controllers to compete with. Because of their widespread use, many techniques have been proposed for their design, namely, for the tuning of the parameters and for the implementation of additional functionalities that improve their performance; see for example [6, 83, 132].

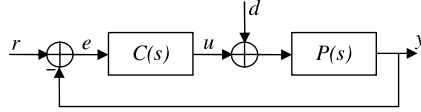


Fig. 2.1 Standard unity-feedback control scheme

A PID controller consists of the sum of three control actions, namely, a control action proportional to the control error, a control action proportional to the integral of the control error, and a control action proportional to the first derivative of the control error. Indeed, the proportional action implements the typical operation of increasing the control variable when the control error is large (with appropriate sign). The integral action is related to the past values of the control error and allows the reduction to zero of the steady-state error when a step reference signal is applied or a constant load disturbance d occurs. The derivative action is based on the predicted future values of the control error and has therefore a great potential in improving the control performance as it can anticipate an incorrect trend of the control error and counteract for it.

In its basic form, the control action can be expressed as

$$u(t) = K_p \left(e(t) + \frac{1}{T_i} \int_0^t e(v) dv + T_d \frac{d}{dt} e(t) \right), \quad (2.1)$$

where $e(t) = r(t) - y(t)$ is the control error (see Figure 2.1), K_p is the proportional gain, T_i is the integral time constant, and T_d is the derivative time constant. The corresponding transfer function is

$$C(s) = \frac{U(s)}{E(s)} = K_p \left(1 + \frac{1}{T_i s} + T_d s \right). \quad (2.2)$$

Actually, the transfer function (2.2) is not proper. In order to make it proper, a filter is usually added to the derivative term (note that this also reduces the detrimental effect of the high-frequency measurement noise), so that

$$C(s) = \frac{U(s)}{E(s)} = K_p \left(1 + \frac{1}{T_i s} + \frac{T_d s}{1 + \frac{T_d}{N} s} \right), \quad (2.3)$$

where the value of N generally assumes a value between 1 and 33, although in the majority of the practical cases, its setting falls between 8 and 16 (usually 10) [1]. Alternatively, the whole control action can be filtered, yielding the following transfer function:

$$C(s) = K_p \left(1 + \frac{1}{T_i s} + T_d s \right) \frac{1}{T_f s + 1}, \quad (2.4)$$

where the time constant T_f has to be selected so that the first-order filter does not influence the dynamics of the PID controller significantly and the high-frequency noise is filtered appropriately at the same time.

It is worth noting at this point that there are other possible configurations for a PID controller. In fact, in addition to Expression (2.2), which is called the *ideal* form (or *non-interacting* form), the three control actions can also be implemented in the so-called *series* or *interacting* form, namely (the filter is omitted for simplicity),

$$C(s) = K_p' \left(\frac{T_i' s + 1}{T_i' s} \right) (T_d' s + 1), \quad (2.5)$$

or, alternatively, in *parallel* form as

$$C(s) = K_p + \frac{K_i}{s} + K_d s. \quad (2.6)$$

Translation formulae can be employed to determine the values of the parameters of an equivalent PID controller in a given form starting from the parameters of the PID controller in another form. However, it has to be stressed that the ideal form is more general than the series form because the controller can be designed with complex conjugate zeros.

2.1.2 Improvements

Modifications of the basic control law (2.1) are usually implemented to cope with practical issues. For example, the derivative action is often applied to the process output y instead of to the control error, so that an impulse in the control signal is avoided when a step signal is applied to the set-point. In this case, the derivative action $u_d(t)$ is expressed as

$$u_d(t) = -\frac{K_p}{T_d} \frac{d}{dt} y(t). \quad (2.7)$$

Thus, a general formula for the derivative action can be written as

$$u_d(t) = \frac{K_p}{T_d} \left(\gamma \frac{d}{dt} r(t) - \frac{d}{dt} y(t) \right), \quad (2.8)$$

where $\gamma = 1$ if the derivative action is applied to the control error and $\gamma = 0$ if the derivative action is applied to the process output.

Further, a set-point weight can be applied also to the proportional action in order to reduce the overshoot in the set-point step response (this is done at the expense of an increase of the rise time), so that the proportional action $u_p(t)$ is expressed as

$$u_p(t) = K_p (\beta r(t) - y(t)), \quad (2.9)$$

where the value of β is selected in the interval $[0, 1]$. The use of a set-point weight is particularly useful when specifications on both set-point following and load disturbance rejection tasks have to be addressed at the same time. Indeed, a fast load

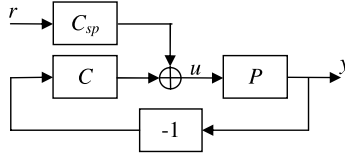


Fig. 2.2 Two-degree-of-freedom PID control scheme

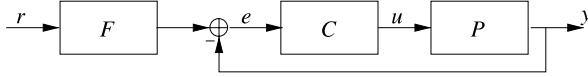


Fig. 2.3 Equivalent two-degree-of-freedom PID control scheme

disturbance rejection is achieved with a controller that provides a large bandwidth, which, in turn, gives an oscillatory set-point step response. By using a set-point weight, the control scheme represented in Figure 2.2 is actually implemented with

$$C(s) = K_p \left(1 + \frac{1}{T_i s} + T_d s \right) \quad (2.10)$$

and

$$C_{sp}(s) = K_p \left(\beta + \frac{1}{T_i s} + \gamma T_d s \right). \quad (2.11)$$

It appears that the load disturbance rejection does not depend on the weight β and therefore can be addressed separately from the set-point following task. Thus, the PID parameters can be selected to achieve a high load disturbance rejection performance, and then the set-point following performance can be recovered by suitably selecting the value of the parameter β . An equivalent control scheme is shown in Figure 2.3, where

$$F(s) = \frac{1 + \beta T_i s + \gamma T_i T_d s^2}{1 + T_i s + T_i T_d s^2}. \quad (2.12)$$

Here it is more apparent that the set-point weight is able to smooth the (step) set-point signal in order to damp the response to a set-point change.

If these modifications of the basic control law are considered, the general so-called *ISA form* (or *beta-gamma*) PID control law can be derived:

$$u(t) = K_p \left(\beta r(t) - y(t) + \frac{1}{T_i} \int_0^t e(\tau) d\tau + T_d \left(\frac{d(\gamma r(t) - y_f(t))}{dt} \right) \right), \quad (2.13)$$

$$\frac{T_d}{N} \frac{dy_f(t)}{dt} = y(t) - y_f(t),$$

where $\beta \in [0, 1]$ and $\gamma \in \{0, 1\}$.

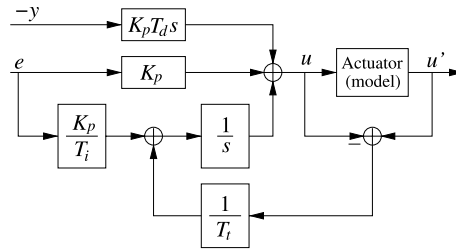


Fig. 2.4 The back-calculation anti-windup scheme

Finally, the integrator windup phenomenon has to be avoided. When a set-point change is applied, the control variable might reach and remain at the actuator saturation limit during the transient response. In this case the system operates as in the open-loop case because the actuator is at its maximum (or minimum) limit, regardless of the process output value. The control error decreases more slowly than in the ideal case (where there is no saturation limits), and therefore the integral term becomes large (it *winds up*). Thus, even when the value of the process variable attains that of the reference signal, the controller still saturates due to the integral term, and this generally leads to large overshoots and long settling time. In order to avoid this, an anti-windup strategy should be implemented. This can be done according to the so-called *conditional integration* technique, where the integral action is frozen when the actuator saturates and, at the same time, the control error and the control variable have the same sign, or according to the so-called *back-calculation* approach shown in Figure 2.4, where the integral action is reduced by a term proportional to the saturation level of the actuator. The parameter T_t , called the tracking time constant, determines the amount of reduction of the integral term.

2.2 Identification

System identification is a topic that has been and is extensively investigated, and many solutions have been proposed in the literature that can be applied in general to industrial processes. In the following sections, methodologies that have been specifically devised for the estimation of the parameters of a integral process are presented, by considering open-loop and closed-loop techniques that can be easily applied in practical cases. Simple continuous-time models are considered because these are commonly employed for the tuning of PID controllers.

2.2.1 Open-loop Identification

Open-loop identification techniques are based on the evaluation of the response of the process to particular signals. They have to be applied starting from an equilibrium point of the system.

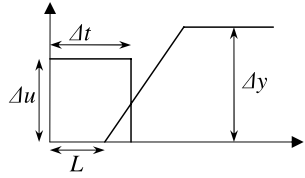


Fig. 2.5 Identification based on the impulse response

2.2.1.1 Using an Impulsive Input

In general, the most employed open-loop identification methods used for industrial system are based on the evaluation of a step response. However, in the case of integral processes, which are not asymptotically stable, the step response would tend to infinity, and this may not be acceptable in practice. An alternative sensible procedure is to apply an impulse to the system. Consider the IPDT system

$$P(s) = \frac{K}{s} e^{-Ls} \quad (2.14)$$

at a steady state (denote the output value as y_0) and apply an impulse of amplitude Δu and duration Δt as the input signal. This is shown in Figure 2.5 together with the corresponding output. The dead time L can be estimated by considering the time interval between the step transition and the time instant when the process output leaves its previous value, namely, $y > y_0$ (without loss of generality, it has been assumed that $\Delta u > 0$ and $K > 0$). It should be noted that in practice the measurement noise needs to be taken into consideration. A simple sensible solution is to define a noise band NB [8] (whose amplitude should be equal to the amplitude of the measurement noise) and to rewrite the condition as $y > y_0 + NB$. The value of K can then be derived, by considering that the value of the process output variation Δy is equal to the area of the impulse input multiplied by K , as

$$K = \frac{\Delta y}{\Delta u \Delta t}. \quad (2.15)$$

The estimation of the parameter K is based just on the steady-state value of the process output, and therefore it is easy to cope with measurement noise. Obviously, the estimation will be perfect when the process dynamics are represented perfectly by expression (2.14). This is not the case if the true process dynamics are different. For example, consider the process

$$P(s) = \frac{1}{s(s+1)} e^{-0.5s}. \quad (2.16)$$

If the open-loop impulse response (plotted as a solid line in Figure 2.6) is evaluated, the following IPDT model is obtained (note that the noise-free case is considered for the sake of simplicity):

$$P(s) = \frac{1}{s} e^{-0.5s}, \quad (2.17)$$

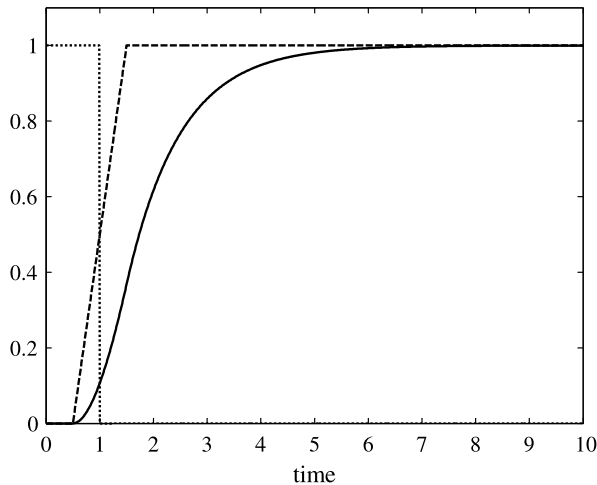


Fig. 2.6 Application of the identification method based on the impulse response. *Dotted line*: impulse input. *Solid line*: process response. *Dashed line*: response of the identified model

which gives the impulse response plotted as a dashed line in Figure 2.6. It turns out that the identification procedure has not captured the dynamics represented by the pole in $s = -1$, and the two responses are therefore somewhat different.

2.2.1.2 Using a Square Wave Input

The gain K can be identified via applying a square wave $u(t)$ with period P and amplitude Δu centred around a nominal value u^* [75]. Since the input function u is discontinuous at the time instants $t_d = P/2, P, 3P/2, \dots$, the output response is continuous but not differentiable at these time instants. The gain K can be therefore computed as

$$K = \frac{\dot{y}(t_d^+) - \dot{y}(t_d^-)}{\Delta u}, \quad (2.18)$$

where $\dot{y}(t_d^+)$ and $\dot{y}(t_d^-)$ are respectively the time derivatives of the process output from the right and the left. The situation is shown in Figure 2.7, where the process $P(s) = 0.1/s$ is taken as an example (the dead time is omitted as it does not affect the identification of K). The main advantage of the method is that, by evaluating the gain at each discontinuity time instant, a time-varying gain can be estimated, and this fact can be exploited in the design of the controller (see [75] for an example related to a batch distillation column). However, it has to be taken into account that the differentiation procedure is very sensitive to the measurement noise and therefore data should be appropriately filtered before applying it.

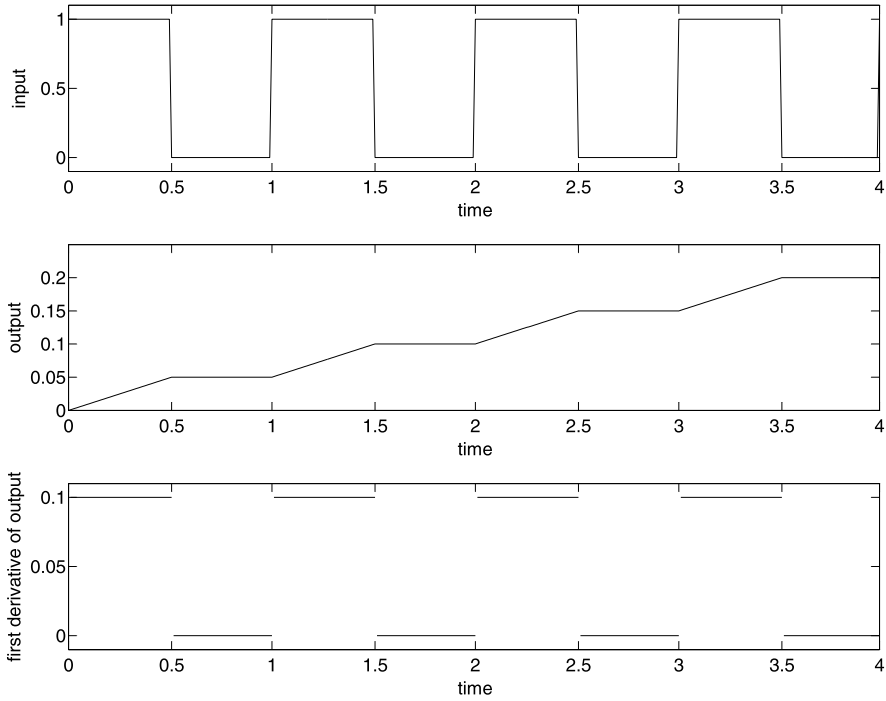


Fig. 2.7 Application of the identification method based on a square wave input

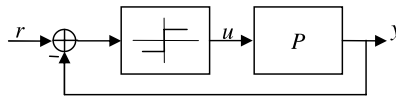


Fig. 2.8 Relay-feedback control scheme

2.2.2 Closed-loop Identification

Closed-loop identification techniques are usually based on the use of a relay feedback controller or, alternatively, on the evaluation of the response to a set-point change. Different methods in these contexts are presented hereafter.

2.2.2.1 Based on the Relay Feedback Methods

The closed-loop identification techniques employed for industrial processes are typically based on a relay-feedback experiment [151] (see Figure 2.8). The rationale of the use of the relay-feedback controller is to evaluate the obtained process output oscillation in order to obtain a nonparametric model of the process [3], namely its ultimate gain K_u and the ultimate frequency ω_u , in analogy with the original idea of

the ultimate sensitivity experiment of Ziegler and Nichols [166], where the control system is led to the stability limit. Then, starting from these parameters, a transfer function of the process can be determined, if necessary.

Standard Relay-feedback Method The original relay-feedback experiment proposed in [3] involves the use of a standard symmetrical relay in order to generate a persistent oscillatory response of the process output. Denoting by h the amplitude of the relay and by A the amplitude of the output oscillations, the value of the ultimate gain can be calculated, by applying the describing function theory, as

$$K_u = \frac{4h}{\pi A}, \quad (2.19)$$

while the value of the ultimate period $P_u = 2\pi/\omega_u$ is simply the period of the obtained output oscillation. It appears that only the amplitude h of the relay has to be selected by the user. This should be done in order to provide an output oscillation of sufficient amplitude to be well distinguished from the measurement noise, but at the same time it should not be too high so that the process is perturbed as less as possible (and the normal production is not interrupted). Indeed, it is worth stressing that the estimation of the output oscillation is sensitive to the measurement noise and therefore some filtering techniques have to be applied [140]. In addition to the advantage of having just one parameter to be selected by the user and of being performed in closed-loop, so that the process is kept close to the set-point value, the main valuable feature of this identification technique is that the identification experiment can start also if the process is not at an equilibrium point. Further, possible load disturbances that might occur during the experiment can be detected easily by the change to asymmetric pulses in the control variable.

In any case, because of the adoption of the describing function theory, the obtained values of the ultimate gain and ultimate period are approximated. As an example, if the process

$$P(s) = \frac{1}{s} e^{-0.2s} \quad (2.20)$$

is considered, the result obtained by employing a relay-feedback controller is shown in Figure 2.9 (note that a set-point step equal to one has been applied at time $t = 0$). By noting that $h = 1$ and $A = 0.205$, the parameters obtained by applying the identification procedure are (see (2.19)) $K_u = 6.21$ and $P_u = 0.82$, while the true ones are $K_u = 7.85$ and $P_u = 0.80$. Actually, the slight difference is usually acceptable if the parameters are employed for the tuning of a PID controller.

The transfer function (2.14) can be determined from the estimated values of the ultimate gain and ultimate period by using the following expressions [26]:

$$L = 0.25 P_u, \quad (2.21)$$

$$K = \frac{4A}{h P_u}. \quad (2.22)$$

When these are applied to the previous example, then $L = 0.2$ and $K = 1$, which are equal to the true values.

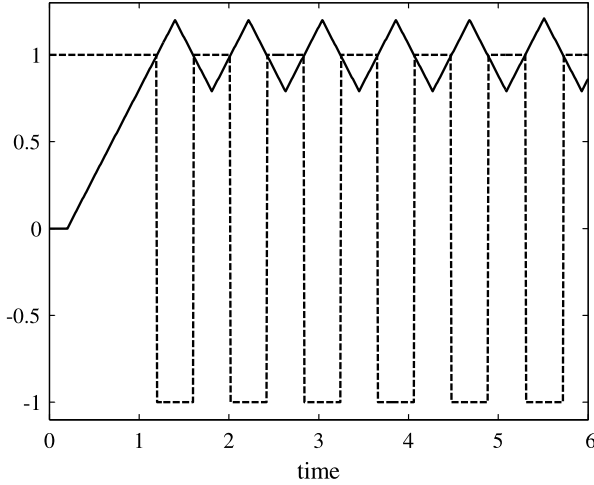


Fig. 2.9 Example of a relay-feedback identification experiment. *Dashed line*: control variable. *Solid line*: process variable

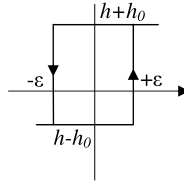


Fig. 2.10 Biased relay with hysteresis

Biased Relay with Hysteresis A biased relay with hysteresis (see Figure 2.10) can also be employed effectively for the estimation of a process transfer function (2.14) [59]. In fact, under an asymmetrical biased relay feedback test (see Figure 2.11), the output response of an IPDT system converges to a limit cycle described as

$$\begin{aligned} y_+(t) &= K(h + h_0)t + K(h - h_0)t_0, & t \in [0, P^+], \\ y_-(t) &= K(h - h_0)(t + t_0) + K(h + h_0)P^+, & t \in [0, P^-], \end{aligned} \quad (2.23)$$

where $y_+(t)$ denotes the monotonically ascending part for $t \in [0, P^-]$, corresponding to $t \in [P^+, P_u]$ in the limit cycle, while $y_-(t)$ denotes the monotonically descending part for $t \in [P^+, P_u]$, and $P_u = P^+ + P^-$ is the oscillation period. Based on these analytical expressions, the process parameters can be determined by evaluating an experiment with a biased relay with hysteresis feedback controller. In particular, the process dead time L can be determined as the time interval to attain the positive peak A^+ of the process output response from a relay switch point in a

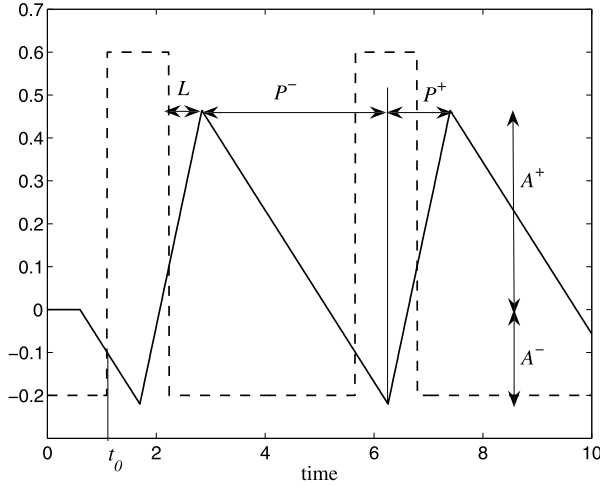


Fig. 2.11 Experiment with a biased relay with a hysteresis feedback controller

negative half period P^- of the relay, and the process gain K can be determined as

$$K = \frac{A^+ - A^-}{(h + h_0)P^+}. \quad (2.24)$$

The use of a biased relay is particularly useful if the system to be estimated is a second-order integral process plus dead time (SOIPDT) described by the transfer function

$$P(s) = \frac{K}{s(Ts + 1)} e^{-Ls}. \quad (2.25)$$

In this case, the analytical expression of the limit cycle can be written as

$$\begin{aligned} y_+(t) &= K(h + h_0)(t - T) + K(h - h_0)t_0 + 2Kh_0TEe^{-t/T}, & t \in [0, P^+], \\ y_-(t) &= K(h - h_0)(t + t_0 - T) + K(h + h_0)P^+ + 2Kh_0TFe^{-t/T}, & t \in (0, P^-], \end{aligned} \quad (2.26)$$

where

$$E = \frac{1 - e^{-P^-/T}}{1 - e^{-P_u/T}}$$

and

$$F = \frac{1 - e^{-P^+/T}}{1 - e^{-P_u/T}}.$$

Based on these expressions, the times to attain the extreme values of $y_+(t)$ and $y_-(t)$, denoted respectively as t_{P^+} and t_{P^-} , can be determined as

$$t_{P^+} = T \ln \frac{2h_0E}{h + h_0} \quad (2.27)$$

and

$$t_{P-} = T \ln \frac{2h_0 F}{h - h_0}. \quad (2.28)$$

Denote the time interval to reach the minimum of $y_+(t)$ from the initial relay switch point in a positive half period of the relay as t_{P+}^* ; then

$$t_{P+} = t_{P+}^* - L, \quad (2.29)$$

and

$$t_{P-} = t_{P-}^* - L, \quad (2.30)$$

where t_{P-}^* is the time interval to reach the maximum of $y_-(t)$ from the initial relay switch point in a negative half period of the relay. By (2.29) and (2.30), we have

$$t_{P+} - t_{P-} = t_{P+}^* - t_{P-}^*. \quad (2.31)$$

Substitute (2.27) and (2.28) into (2.31); then

$$\ln \frac{h_0 - h}{h_0 + h} + \ln \frac{1 - e^{-P^-/T}}{1 - e^{-P^+/T}} = \frac{t_{P+}^* - t_{P-}^*}{T}. \quad (2.32)$$

Note that the process response at the oscillation frequency can be formulated as

$$P(j\omega_u) = \frac{\int_0^{P_u} y(t) e^{-j\omega_u t} dt}{\int_0^{P_u} u(t) e^{-j\omega_u t} dt} = A_u e^{j\varphi_u}. \quad (2.33)$$

Substitute the process model (2.25) into (2.33); then

$$\frac{K}{\omega_u \sqrt{T^2 \omega_u^2 + 1}} = A_u \quad (2.34)$$

and

$$-L\omega_u - \frac{\pi}{2} - \arctan(T\omega_u) = \varphi_u. \quad (2.35)$$

It can be easily derived that

$$K = A_u \omega_u \sqrt{T^2 \omega_u^2 + 1} \quad (2.36)$$

and

$$L = -\frac{1}{\omega_u} \left[\varphi_u + \frac{\pi}{2} + \arctan(T\omega_u) \right]. \quad (2.37)$$

In case $L/T > 1$, $y_+(t)$ can decrease monotonically for $t \in [0, P^+]$, while $y_-(t)$ can increase monotonically for $t \in [0, P^-]$. Thus, there exists

$$t_{P+}^* = t_{P-}^* = L. \quad (2.38)$$

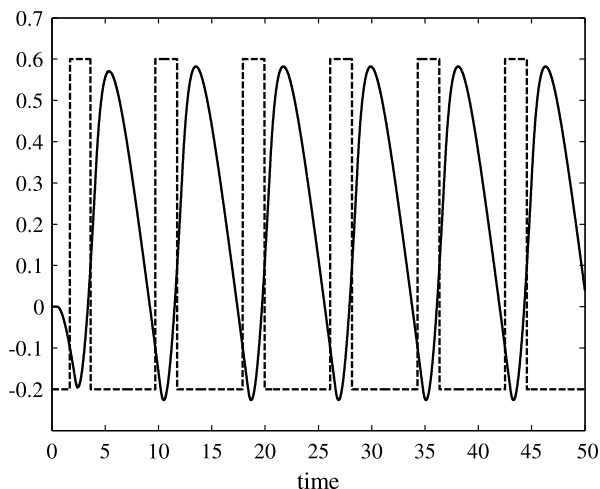


Fig. 2.12 Experiment for the estimation of a SOIPDT process

In this case, the process time constant can be derived from (2.37) as

$$T = \frac{1}{\omega_u} \tan\left(-L\omega_u - \frac{\pi}{2} - \varphi_u\right), \quad (2.39)$$

and the process gain can be determined straightforward from (2.36). However, the value of T cannot be determined from (2.39) if

$$\tan\left(-L\omega_u - \frac{\pi}{2} - \varphi_u\right) < 0. \quad (2.40)$$

The algorithm for the identification of the SOIPDT process (2.25) can be summarised as follows [59]:

1. Measure P^+ , P^- , t_{p+}^* , and t_{p-}^* from the limit cycle.
2. Compute $P(j\omega_u)$ from (2.33).
3. Compute the process dead time from (2.38) and check whether (2.40) is satisfied. If yes, go to step 6.
4. Compute the process time constant T from (2.39) and check whether $L/T < 1$ is satisfied. If yes, go to step 6.
5. Determine the process gain K from (2.36). If both (2.40) and $L/T < 1$ are not satisfied, then terminate.
6. Determine T from (2.32) by applying the Newton–Raphson iteration method. Set $T = t_{p+}^*$ (or $T = t_{p-}^*$) as the initial estimation of T .
7. Determine the process gain K from (2.36).
8. Determine the process dead time L from (2.37).

As an example of this algorithm, the process (2.16) is considered. The result of the application of the biased relay feedback control scheme is shown in Figure 2.12. The

following parameters are obtained: $t_{P+}^* = 0.8$, $t_{P-}^* = 1.76$, $P^+ = 2.04$, $P^- = 6.14$, $P_u = 8.18$, (namely, $\omega_u = 0.77$), $A_u = 1.04$. By applying the algorithm, the process parameters are estimated correctly.

An alternative approach for the estimation of the parameters of a SOIPDT process has been proposed in [35]. The method is based on the application of the relay feedback controller to a first-order-plus-dead-time (FOPDT) process described by the following transfer function:

$$P(s) = \frac{K}{Ts + 1} e^{-Ls}. \quad (2.41)$$

In this case, the process parameters can be estimated by applying the following formulae, which are based again on the describing function analysis:

$$K = \frac{a_0}{u_0}, \quad (2.42)$$

$$T = \frac{P_u}{2\pi \frac{A^+ - A^-}{2}} \sqrt{K^2(\alpha^2 + \beta^2) - \left(\frac{A^+ - A^-}{2}\right)^2}, \quad (2.43)$$

$$L = \frac{P_u}{2\pi} \left[\pi - \tan^{-1} \left(\frac{2\pi T}{P_u} \right) + \tan^{-1} \left(\frac{\alpha}{\beta} \right) \right], \quad (2.44)$$

where

$$\alpha = \frac{-4h_0\varepsilon}{\pi \frac{A^+ - A^-}{2}}, \quad (2.45)$$

$$\beta = \frac{h}{\pi \frac{A^+ - A^-}{2}} \left(\sqrt{\left(\frac{A^+ - A^-}{2}\right)^2 - (a_0 - \varepsilon)^2} + \sqrt{\left(\frac{A^+ - A^-}{2}\right)^2 - (a_0 + \varepsilon)^2} \right), \quad (2.46)$$

and a_0 and u_0 are the values of the DC components of the oscillations at the process output and input. In case the process is described by a SOIPDT transfer function, in principle it is sufficient to differentiate the output of the relay and then apply the preceding formulae (2.42)–(2.44). Obviously, differentiating the relay output gives impulses at the zero crossings that are not acceptable in practical cases because of the actuator constraints. In order to cope with this problem, the ideal impulses can be substituted by pulses with finite amplitude and short pulse width. Actually, this introduces an approximation that might significantly affect the estimation result.

It is worth stressing that, when a relay feedback controller is employed, some filtering techniques should be applied because the estimation of the output oscillation is sensitive to the measurement noise. Furthermore, the use of an asymmetrical relay represents a sort of disturbance to the process since it causes the operating point to drift.

2.2.2.2 Based on the Closed-loop Step Responses

A closed-loop identification method which is an alternative to the use of a relay feedback controller consists of evaluating the set-point step response of the IPDT

process (2.14) with simple proportional controller $C(s) = K_p$ [115]. In this case, the closed-loop transfer function is (see Figure 2.1)

$$\frac{Y(s)}{R(s)} = \frac{K'e^{-Ls}}{s + K'e^{-Ls}}, \quad (2.47)$$

where

$$K' = K_p K. \quad (2.48)$$

By using a first-order Padé approximation, namely $e^{-Ls} \cong (1 - 0.5Ls)/(1 + 0.5Ls)$, Expression (2.47) can be rewritten as

$$\frac{Y(s)}{R(s)} = \frac{K'(1 + 0.5Ls)e^{-Ls}}{0.5\frac{L}{K'}s^2 + (\frac{1}{K'} - 0.5L)s + 1} \quad (2.49)$$

or, equivalently,

$$\frac{Y(s)}{R(s)} = \frac{K'(1 + 0.5Ls)e^{-Ls}}{\tau_e^2 s^2 + 2\tau_e \zeta s + 1} \quad (2.50)$$

with

$$\tau_e = \sqrt{\frac{L}{2K'}} \quad (2.51)$$

and

$$\zeta = \sqrt{\frac{K'}{2L}} \left(\frac{1}{K'} - \frac{L}{2} \right). \quad (2.52)$$

The effective time constant τ_e and the damping coefficient ζ of the closed-loop system can be estimated by considering the closed-loop response parameters y_{M1} , y_{m1} , y_{M2} , y_∞ (namely, the first peak value, the first minimum value, the second peak value, and the steady-state value) and Δt as shown in Figure 2.13. In particular, the following formulae can be employed [26]:

$$\zeta = -\frac{\ln \frac{y_{M2} - y_\infty}{y_{M1} - y_\infty}}{\sqrt{4\pi^2 + \left(\ln \frac{y_{M2} - y_\infty}{y_{M1} - y_\infty} \right)^2}}, \quad (2.53)$$

or, alternatively,

$$\zeta = -\frac{\ln \frac{y_\infty - y_{m1}}{y_{M1} - y_\infty}}{\sqrt{\pi^2 + \left(\ln \frac{y_\infty - y_{m1}}{y_{M1} - y_\infty} \right)^2}}, \quad (2.54)$$

and

$$\tau_e = \frac{\Delta t}{\pi} \sqrt{1 - \zeta^2}. \quad (2.55)$$

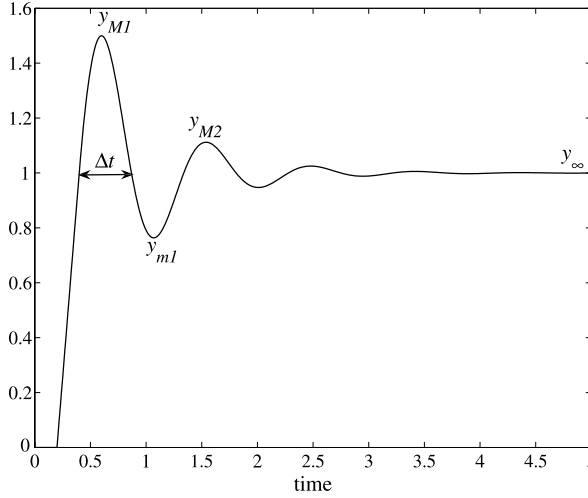


Fig. 2.13 Experiment for the estimation of a SOIPDT process

The values of L and K' (and consequently of K) can be eventually determined, by solving Equations (2.51) and (2.52), as

$$L = \frac{2.828\Delta t}{\pi} \sqrt{0.5 + \zeta^2 - \sqrt{\zeta^2(1 + \zeta^2)}} \sqrt{1 - \zeta^2}, \quad (2.56)$$

$$K = \frac{1.414\pi}{\Delta t \sqrt{1 - \zeta^2}} \sqrt{0.5 + \zeta^2 - \sqrt{\zeta^2(1 + \zeta^2)}}. \quad (2.57)$$

It is worth noting that the value of the proportional gain of the controller has to be sufficiently high to provide an oscillatory set-point step response.

As an illustrative example of application of the identification procedure, consider process (2.20). If a proportional feedback controller $K_p = 5$ is employed, the resulting set-point step response is shown in Figure 2.13 with $y_{M1} = 1.5$, $y_{m1} = 0.76$, $y_{M2} = 1.11$, and $y_\infty = 1$. By applying either (2.53) or (2.54) we have $\zeta = 0.23$, and, as a consequence, from (2.56), (2.57), and (2.48) the resulting values of the process parameters are $K = 1.09$ and $L = 0.23$. The slight discrepancy between the true and estimated values is due to the Padé approximation.

2.3 Tuning Methods

A large number of tuning methods have been proposed in literature over the last seventy years. They are based on different approaches and aim at solving different control problems. In fact, as it has already been mentioned in Section 2.1, there are different (possibly conflicting) control tasks that have to be addressed in practical cases. In particular, set-point following and/or load disturbance rejection are usually of main concern. In general, a good load disturbance rejection performance is

achieved with a high-gain controller, which gives an oscillatory set-point step response on the other side. If both specifications have to be considered, the problem can be solved by employing a set-point weight. It is worth stressing at this point that, although the use of a set-point weight yields a two-degree-of-freedom control system, its use is addressed in this part of the book because the two controllers (C and F) in Figure 2.3 are actually strongly correlated. In Part II of the book, in a context different from PID controllers, the two controllers are designed separately in a two-degree-of-freedom scheme.

In addition to the performance in the set-point following and/or load disturbance rejection tasks, the performance in the filtering of measurement noise, the robustness of the control scheme and the control effort have to be considered as well in the selection of the PID parameters. For this reason, it is difficult to make the best choice among the many tuning rules that are available.

In the following subsections, instead of providing a comprehensive review of all the tuning rules that are available for integral processes (see [83] for this purpose), different approaches with the aim of showing the peculiarities of integral processes are highlighted.

2.3.1 Empirical Formulae

Empirical formulae for the tuning of the PID controllers have been devised soon after PID controllers appeared in the industry at the beginning of the last century. The most well-known formulae are those devised by Ziegler and Nichols in the 1940s [166]. There are two kinds of formulae that are based respectively on the parametric model (2.14) and on the nonparametric model given by the ultimate gain K_u and the ultimate frequency ω_u . They are shown in Tables 2.1 and 2.2, respectively. It is worth noting that the Ziegler–Nichols tuning rules aim at providing a good load disturbance rejection performance (in particular, a quarter decay ratio in the load disturbance step response), and this implies that the damping ratio of the closed-loop system is in general too low to achieve a satisfactory set-point following performance (namely, the step response is too oscillatory with a big overshoot). As already mentioned, this issue can be addressed by employing a set-point weight for the proportional action. As an example, consider the process

$$P(s) = \frac{0.0506}{s} e^{-6s}. \quad (2.58)$$

By applying the PID controller tuning rule shown in Table 2.1, the parameters are $K_p = 3.95$, $T_i = 12$, and $T_d = 3$. The resulting set-point and load disturbance rejection step response is shown in Figure 2.14 as a solid line. If a set-point weight $\beta = 0.4$ is employed, the result obtained is the one shown with a dashed line. If Table 2.2 is used to determine the PID parameters (note that $K_u = 5.19$ and $P_u = 24$), the parameters are $K_p = 3.11$, $T_i = 12$, and $T_d = 3$. The corresponding results (obtained again with and without the set-point weight) are plotted in Figure 2.15. As it can be easily expected by evaluating the controller parameters, the method based

Table 2.1 Ziegler–Nichols tuning rules based on a parametric model

Controller	K_p	T_i	T_d
P	$\frac{1}{K L}$	–	–
PI	$\frac{0.9}{K L}$	$3L$	–
PID	$\frac{1.2}{K L}$	$2L$	$\frac{L}{2}$

Table 2.2 Ziegler–Nichols tuning rules based on a non-parametric model

Controller	K_p	T_i	T_d
P	$0.5K_u$	–	–
PI	$0.4K_u$	$0.8P_u$	–
PID	$0.6K_u$	$0.5P_u$	$0.125P_u$

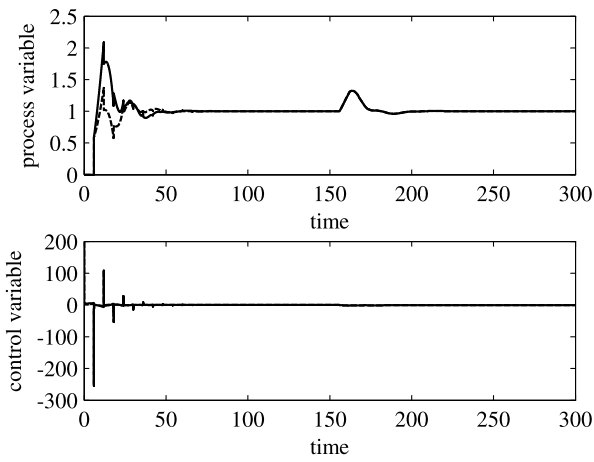


Fig. 2.14 Results obtained with the Ziegler–Nichols tuning rules based on a parametric model of the process. *Solid line*: PID controller with no set-point weight. *Dashed line*: PID controller with set-point weight

on the nonparametric model of the process provides a less oscillatory response. In any case, the use of a set-point weight is actually essential in reducing the excessive overshoot that occurs because of the aggressive tuning conceived to achieve a fast load disturbance rejection.

2.3.2 Analytical Methods

In contrast to empirical tuning rules, analytical methods are based on the determination of the controller parameters by exploiting explicitly the expressions that involve the transfer function of the closed-loop system.

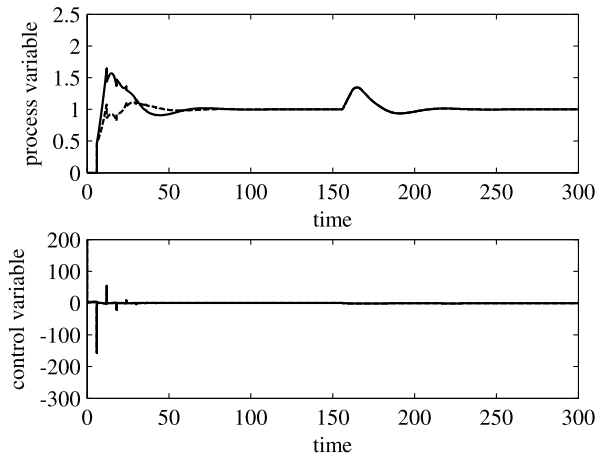


Fig. 2.15 Results obtained with the Ziegler–Nichols tuning rules based on a nonparametric model of the process. *Solid line*: PID controller with no set-point weight. *Dashed line*: PID controller with set-point weight

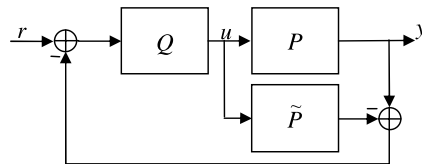


Fig. 2.16 The general Internal Model Control scheme

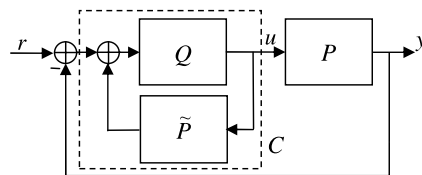


Fig. 2.17 The equivalent unity-feedback control scheme

2.3.2.1 Internal Model Control

Internal Model Control (IMC) [76] is a well-known control design approach where the trade-off between nominal performance and robustness is explicitly addressed. This is obtained by including a model of the process in the controller implementation, according to the scheme of Figure 2.16, where \tilde{P} denotes the model of the process P , and the controller Q determines the value of the control variable u . Note that this scheme is equivalent to the unity-feedback scheme of Figure 2.1 by simply selecting (see Figure 2.17)

$$C(s) = \frac{Q(s)}{1 - \tilde{P}(s)Q(s)}. \quad (2.59)$$

The design of the controller is in general performed by considering $Q(s) = \tilde{Q}(s)F(s)$ and by selecting $\tilde{Q}(s)$ in order to achieve an optimal performance for a given input disregarding the model uncertainties (namely, by considering $\tilde{P}(s) = P(s)$) and input constraints. Then, $F(s)$ is selected as a low-pass filter of an appropriate order in order to achieve robust stability and robust performance. In particular, $\tilde{Q}(s)$ can be determined to minimise the integrated square error (ISE)

$$\int_0^\infty e^2(t) dt. \quad (2.60)$$

This is obtained by factoring the model $\tilde{P}(s)$ into two parts:

$$\tilde{P}(s) = \tilde{P}_+(s)\tilde{P}_-(s), \quad (2.61)$$

where $\tilde{P}_+(s)$ is the all-pass portion of the transfer function ($\tilde{P}_+(0) = 1$) including all the RHP zeros and delays of $\tilde{P}(s)$, having the form

$$\tilde{P}_+(s) = e^{-Ls} \prod_i \frac{-\alpha_i s + 1}{\alpha_i s + 1}, \quad (2.62)$$

where α_i^{-1} are all the RHP zeros, and L is the dead time.

Alternatively, if it is desired to minimise the integrated absolute error (IAE)

$$\int_0^\infty |e(t)| dt, \quad (2.63)$$

$\tilde{P}_+(s)$ in the factorisation (2.61) should be chosen as

$$\tilde{P}_+(s) = e^{-Ls} \prod_i (-\alpha_i s + 1). \quad (2.64)$$

Then, $\tilde{Q}(s) = \tilde{P}_-^{-1}(s)$. At this point, $F(s)$ has to be selected in order to have a proper controller $Q(s)$. With the inclusion of the filter, the transfer function of the closed-loop system of Figure 2.16 becomes $P(s)\tilde{Q}(s)F(s)$ (again, by considering $\tilde{P}(s) = P(s)$). Thus, in order to achieve a null steady-state error in the presence of a step set-point signal, it has to be $F(0) = 1$. In this context, a natural choice is to select

$$F(s) = \frac{1}{(\lambda s + 1)^n}, \quad (2.65)$$

where the order n is such that the controller $Q(s)$ is proper. In order to have a null steady-state error when a ramp signal is applied to the set-point, in addition to the requirement $F(0) = 1$, the following expressions needs to be satisfied as well:

$$\left. \frac{d}{ds} (\tilde{P}(s)Q(s)) \right|_{s=0} = 0$$

Table 2.3 IMC-based PID tuning rules

Approximation	$K_p K$	T_i	T_d	T_f	Comments
$e^{-Ls} \cong 1 - Ls$	$\frac{2(L+\lambda)}{2L^2+4\lambda L+\lambda^2}$	$2(L+\lambda)$	–	$\frac{L\lambda^2}{2L^2+4\lambda L+\lambda^2}$	ISE optimal
$e^{-Ls} \cong 1 - Ls$	$\frac{L+2\lambda}{(L+\lambda)^2}$	$L+2\lambda$	–	–	IAE optimal
$e^{-Ls} \cong \frac{1-\frac{L}{2}s}{1+\frac{L}{2}s}$	$\frac{3L+2\lambda}{2L^2+4\lambda L+\lambda^2}$	$3L+2\lambda$	$\frac{2L(L+\lambda)}{3L+2\lambda}$	$\frac{L\lambda^2}{2L^2+4\lambda L+\lambda^2}$	ISE optimal
$e^{-Ls} \cong \frac{1-\frac{L}{2}s}{1+\frac{L}{2}s}$	$\frac{2}{L+\lambda}$	$2(L+\lambda)$	$\frac{L(L+2\lambda)}{2(L+\lambda)}$	–	IAE optimal

or, equivalently,

$$\left. \frac{d}{ds} (\tilde{P}_+(s)F(s)) \right|_{s=0} = 0.$$

A possible solution is

$$F(s) = \frac{(2\lambda - \tilde{P}'_+(0))s + 1}{(\lambda s + 1)^2}. \quad (2.66)$$

By restricting the analysis to IPDT processes (2.14), it has to be stressed that, in order to have a null steady-state error with a constant load disturbance, it is necessary for the controller to have a pole at the origin. This corresponds to having a null steady-state error when a ramp signal is applied to the set-point, and therefore the filter transfer function (2.66) has to be considered. Then, if the dead time is approximated as

$$e^{-Ls} \cong 1 - Ls \quad (2.67)$$

and the IMC design procedure is applied, $C(s)$ becomes a PI controller with or without an output filter, respectively, depending on whether the factorisation (2.62) or (2.64) is applied. If the dead time is approximated as

$$e^{-Ls} \cong \frac{1 - \frac{L}{2}s}{1 + \frac{L}{2}s}, \quad (2.68)$$

then $C(s)$ becomes a PI controller with or without an output filter, respectively, depending on whether the factorisation (2.62) or (2.64) is applied. Thus, the application of the IMC design naturally yields the tuning rules shown in Table 2.3 [108], where the only parameter to be selected by the user is λ , which handles the trade-off between aggressiveness and robustness (and control activity). Indeed, increasing the value of λ implies that the closed-loop time constant increases and the robustness of the control system to plant/model mismatch increases. Conversely, decreasing the value of λ implies that the speed of response increases but the system is less robust. Different practical recommendations for the choice of λ have been proposed in the literature. For example, the advice $\lambda > L/4$ or $\lambda > L/2$ is given in [108] corresponding to the factorisation form (2.62) or (2.64), while the suggestion $\lambda = L\sqrt{10}$ is given in [2]. It is worth stressing that if the PID controller has a form

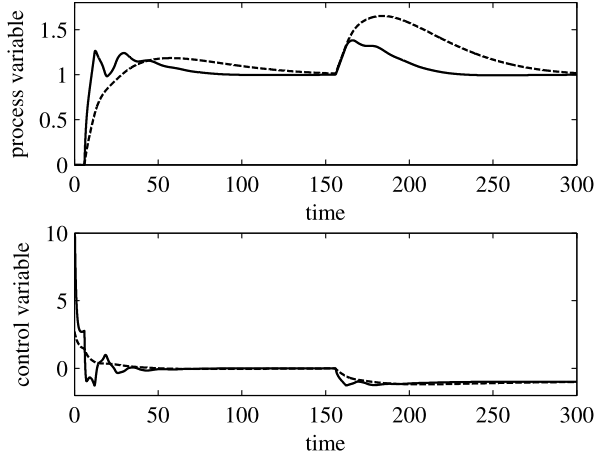


Fig. 2.18 Results obtained with the IMC-based tuning rules. *Solid line:* $\lambda = 6$. *Dashed line:* $\lambda = 18.97$

different from the output filtered ideal one (2.4), simple conversion formulae can be employed [15].

As an illustrative example, consider again process (2.58). By applying the tuning rule that yields a PID controller with an output filter and by initially selecting $\lambda = L = 6$, the parameters are $K_p = 2.35$, $T_i = 30$, $T_d = 4.8$, and $T_f = 0.86$. The response to a set-point and load disturbance step signals is shown in Figure 2.18 as a solid line. Conversely, by selecting $\lambda = L\sqrt{10} = 18.97$, it is $K_p = 1.25$, $T_i = 55.95$, $T_d = 5.36$, and $T_f = 2.43$. The corresponding set-point and load disturbance step responses are plotted again in Figure 2.18 as a dashed line. As expected, a bigger value of λ yields a less aggressive and more robust control system, namely, the overshoot in the set-point step response is reduced, the rise time is increased, and the control effort is reduced as well. Conversely, a more sluggish load disturbance response is obtained.

2.3.2.2 Matching the Coefficients of the Closed-loop Transfer Function

If just the set-point following performance is addressed, a simple method to tune the PID controller is to match the coefficients of the numerator and denominator polynomial of the closed-loop transfer function [14]. If an IPDT process transfer function (2.14) is considered and a PID controller (2.2) is employed, the closed-loop transfer function from the set-point r to the output y is

$$\frac{Y(s)}{R(s)} = \frac{(K_1 q + K_2 + K_3 q^2)e^{-q}}{q^2 + (K_1 q + K_2 + K_3 q^2)e^{-q}}, \quad (2.69)$$

where

$$q = Ls, \quad (2.70)$$

$$K_1 = K_p K L, \quad (2.71)$$

$$K_2 = \frac{K_1 L}{T_i}, \quad (2.72)$$

$$K_3 = K_1 \frac{T_d}{L}. \quad (2.73)$$

By using the first-order Padè approximation for the exponential term at the denominator, Expression (2.69) becomes

$$\frac{Y(s)}{R(s)} = \frac{(K_1 q + K_2 + K_3 q^2)(1 + 0.5q)e^{-q}}{(1 + 0.5q)q^2 + (K_1 q + K_2 + K_3 q^2)(1 - 0.5q)}. \quad (2.74)$$

By imposing that this closed-loop transfer function is equal to one, it results

$$K_1 = 1, \quad (2.75)$$

$$K_2 = 0, \quad (2.76)$$

$$K_3 = 0.5, \quad (2.77)$$

that is (see (2.71)–(2.73)),

$$K_p = \frac{1}{K L}, \quad (2.78)$$

$$T_i = \infty, \quad (2.79)$$

$$T_d = 0.5L. \quad (2.80)$$

Indeed, a PD controller results. This is in accordance with the intuition that a pole at the origin of the complex plane to ensure a null steady-state error is already present in the process transfer function. In order to employ the integral action in any case (for example to cope with possible load disturbances), it is sufficient to impose that the closed-loop transfer function (2.74) is equal to $\alpha > 1$ (note that if $\alpha = 1$, the same tuning rules as before are obtained). This is reasonable because the steady-state error will be zero in any case (because of the presence of the integrator) and because with a PI or PID controller an overshoot occurs in any case in the set-point step response. Thus, by considering α as a tuning parameter, the following expressions are obtained:

$$(1 - \alpha)K_1 + 0.5(1 + \alpha)K_2 = 0, \quad (2.81)$$

$$0.5(1 + \alpha)K_1 + (1 - \alpha)K_3 = \alpha, \quad (2.82)$$

$$(1 + \alpha)K_3 = \alpha, \quad (2.83)$$

which yields

$$K_p = \frac{1}{K L} \frac{4\alpha^2}{(1 + \alpha^2)}, \quad (2.84)$$

$$T_i = 0.5L \left(\frac{1+\alpha}{\alpha-1} \right), \quad (2.85)$$

$$T_d = 0.25L \left(\frac{1+\alpha}{\alpha} \right). \quad (2.86)$$

If a PI controller is considered, by following the same reasoning as before the following rules are obtained:

$$K_p = \frac{1}{KL} \frac{2\alpha}{1+\alpha}, \quad (2.87)$$

$$T_i = 0.5L \left(\frac{1+\alpha}{\alpha-1} \right). \quad (2.88)$$

It appears that all the PID parameters depend on the value of α which has to be selected conveniently. In [14] it is suggested to choose $\alpha = 1.25$, namely, for the PID controller:

$$K_p = \frac{1.2346}{KL}, \quad (2.89)$$

$$T_i = 4.5L, \quad (2.90)$$

$$T_d = 0.45L. \quad (2.91)$$

As an illustrative example of the method, consider the process (2.58). By applying (2.89)–(2.91) the following parameters are determined: $K_p = 4.067$, $T_i = 27$, and $T_d = 2.7$. The resulting set-point and load disturbance unit step responses are shown as a solid line in Figure 2.19. They are compared with the results obtained by using a PI controller with $K_p = 3.66$ and $T_i = 27$ (see (2.87)–(2.88)), shown as a dashed line, and with the results obtained by using a PD controller with $K_p = 3.29$ and $T_d = 3$ (see (2.78)–(2.80)), shown as a dotted line. In the cases where the derivative action has been employed, a first-order filter has been applied, but its time constant has been selected so that its dynamics are actually negligible (note that the derivative filter has not been considered explicitly in the derivation of the tuning rules). This explains the large spikes in the control signal (no saturation of the actuator has been considered in order to avoid biasing the result). Further, as expected, the use of the PD controller provides a better set-point step response but exhibits a steady-state error in the presence of a constant load disturbance. The PID controller performs better than the PI controller, but a large overshoot appears in all of the cases.

2.3.2.3 Direct-synthesis-based Design

With respect to the method described in Section 2.3.2.2, an increase in the performance can be expected if a filtered PID controller (possibly with set-point weight) is employed. In this context, the method based on direct synthesis proposed in [107]

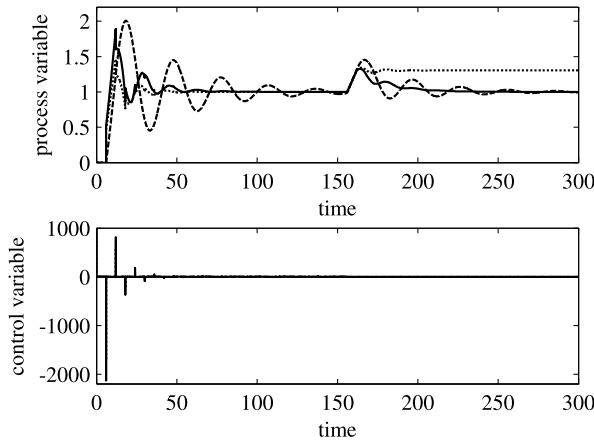


Fig. 2.19 Results obtained with the method based on matching the coefficients of the closed-loop transfer function. *Solid line*: PID controller. *Dashed line*: PI controller. *Dotted line*: PD controller

can be applied. In fact, if the scheme of Figure 2.1 is considered and if an appropriate desired closed-loop transfer function is selected, then the controller transfer function determined analytically has the required structure. Indeed, if the IPDT process (2.14) is considered and the desired closed-loop transfer function is selected as

$$\left(\frac{Y(s)}{R(s)}\right)_d = \frac{(\eta s + 1)e^{-Ls}}{(\lambda s + 1)^2}, \quad (2.92)$$

then, the corresponding controller transfer function can be determined as

$$C(s) = \frac{1}{P(s)} \frac{\left(\frac{Y(s)}{R(s)}\right)_d}{1 - \left(\frac{Y(s)}{R(s)}\right)_d} = \frac{s}{K} \frac{(\eta s + 1)}{[(\lambda s + 1)^2 - (\eta s + 1)e^{-Ls}]}. \quad (2.93)$$

By applying the first-order Padè approximation $e^{-Ls} \cong (1 - \frac{L}{2}s)/(1 + \frac{L}{2}s)$ and by selecting $\eta = 2\lambda + L$, from (2.93) an output-filtered PID controller (2.4) is obtained, where

$$K_p = \frac{2\lambda + 1.5L}{K(\lambda^2 + 2\lambda L + 0.5L^2)}, \quad (2.94)$$

$$T_i = 2\lambda + 1.5L, \quad (2.95)$$

$$T_f = \frac{0.5\lambda^2 L}{\lambda^2 + 2\lambda L + 0.5L^2}. \quad (2.96)$$

The same method can be applied also to SOIPDT processes (2.25). In this case, the desired closed-loop transfer function has to be selected as

$$\left(\frac{Y(s)}{R(s)}\right)_d = \frac{(\eta_2 s^2 + \eta_1 s + 1)e^{-Ls}}{(\lambda s + 1)^3}, \quad (2.97)$$

so that the controller is obtained as

$$C(s) = \frac{1}{P(s)} \frac{\left(\frac{Y(s)}{R(s)}\right)_d}{1 - \left(\frac{Y(s)}{R(s)}\right)_d} = \frac{s(Ts + 1)}{K} \frac{(\eta_2 s^2 + \eta_1 s + 1)}{[(\lambda s + 1)^3 - (\eta_2 s^2 + \eta_1 s + 1)e^{-Ls}]}. \quad (2.98)$$

By using again a first-order Padé approximation, the controller transfer function becomes a PID controller in series with a lead/lag compensator:

$$C(s) = K_p \left(1 + \frac{1}{T_i s} + T_d s \right) \frac{(as + 1)}{(bs + 1)}, \quad (2.99)$$

where

$$K_p = \frac{\eta_1}{K(3\lambda^2 + 1.5\lambda L + 0.5\eta_1 L - \eta_2)}, \quad (2.100)$$

$$T_i = \eta_1, \quad (2.101)$$

$$T_d = \frac{\eta_2}{\eta_1}, \quad (2.102)$$

$$T_f = \frac{0.5\lambda^2 L}{\lambda^2 + 2\lambda L + 0.5L^2}, \quad (2.103)$$

$$a = 0.5L, \quad (2.104)$$

$$b = \frac{0.5\lambda^3 L}{T(3\lambda^2 + 1.5\lambda L + 0.5L\eta_1 - \eta_2)}, \quad (2.105)$$

$$\eta_1 = 3\lambda + L, \quad (2.106)$$

$$\eta_2 = \frac{(0.5L - T)\lambda^3 + (3T^2 - 1.5LT)\lambda^2 + 3LT^2\lambda + 0.5L^2T^2}{T(0.5L + T)}. \quad (2.107)$$

It appears that for both IPDT and SOIPDT processes, there is just one tuning parameter λ which handles the trade-off between aggressiveness and robustness. In [107] it is suggested to select λ in the range $[0.8L, 3L]$. Furthermore, it is suggested to use the set-point weight β in the range of 0.3–0.4 to reduce the overshoot in the step response.

As an illustrative example, by considering again process (2.58), the following parameters are determined, by applying (2.94)–(2.96) with $\lambda = L = 6$: $K_p = 3.29$, $T_i = 21$, $T_d = 2.57$, $T_f = 0.86$. The set-point weight has been fixed to 0.3. The resulting set-point and load disturbance unit step responses are shown in Figure 2.20.

2.3.3 Frequency-domain Methods

Tuning methods can also be developed by considering the frequency response of the system. Some examples are presented in the following subsections.

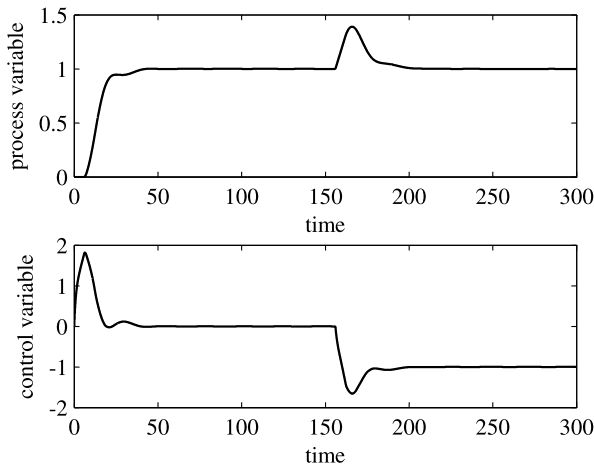


Fig. 2.20 Results obtained with the direct-synthesis-based design method

2.3.3.1 Based on the Maximum Peak-resonance Specification

The method proposed in [101] is based on a specification of a maximum peak resonance and is derived from the analysis of the Nichols chart of the series of the controller and of the process. In fact, with an integral process, the open-loop frequency response presents a phase maximum (see Figure 2.21). In this context, the controller parameters can be selected such that this maximum is located on the right-most point of the ellipse corresponding to the selected maximum peak resonance. Thus, the method can handle at the same time the maximum peak overshoot and the minimum phase and gain margins.

By considering a SOIPDT process (2.25) and a PI controller

$$C(s) = K_p \left(1 + \frac{1}{T_i s} \right), \quad (2.108)$$

specifying that the phase maximum (achieved at the frequency ω_{\max}) of the open-loop frequency response $L(s) = C(s)P(s)$ is located at the right most point (A_{\max}, ϕ_{\max}) of the contour corresponding to the desired maximum peak resonance M_r , yields the following system of three equations and three unknowns (K_p, T_i, ω_{\max}):

$$\left. \frac{\partial \arg L(j\omega)}{\partial \omega} \right|_{\omega=\omega_{\max}} = 0, \quad (2.109)$$

$$\arg L(j\omega_{\max}) = \phi_{\max}, \quad (2.110)$$

$$|L(j\omega_{\max})| = A_{\max}. \quad (2.111)$$

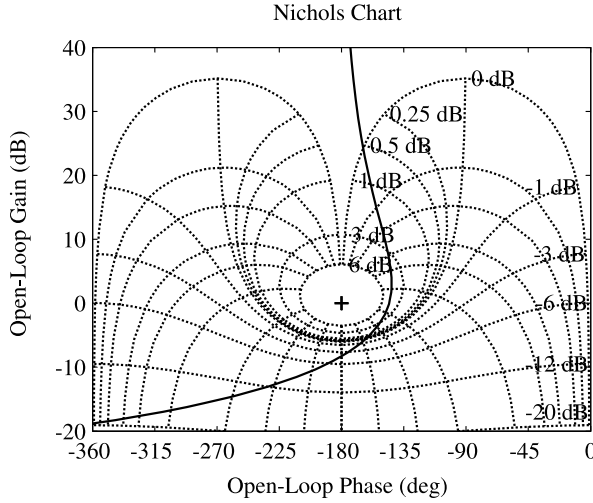


Fig. 2.21 Example of a Nichols chart for an integral process in series with a PI controller

A simple expression of the solution of this system can be obtained by approximating the $\arctan(x)$ as

$$\arctan(x) \cong \begin{cases} \frac{\pi}{2} - \frac{1}{x} & \text{if } x > 1, \\ x & \text{if } x \leq 1. \end{cases} \quad (2.112)$$

In this way the following expressions are obtained:

$$T_i = \frac{16(T + L)}{(2\phi_{\max} + \pi)^2}, \quad (2.113)$$

$$K_p = \frac{T_i A_{\max}}{K} \left[\frac{T_i^2 \omega_{\max}^6 + \omega_{\max}^4}{T_i^2 \omega_{\max}^2 + 1} \right]^{\frac{1}{2}}, \quad (2.114)$$

$$\omega_{\max} = \left[\frac{1}{T_i(T + L)} \right]^{\frac{1}{2}}. \quad (2.115)$$

In order to achieve a good compromise between the set-point following and the load disturbance rejection performance, it is suggested to select $M_r = 5$ dB (which corresponds to $A_{\max} = 1.21$ and $\phi_{\max} = -2.55$ rad). If a PID controller is employed, it has to be selected with transfer function

$$C(s) = K_p \left(\frac{T_i s + 1}{T_i s} \right) \frac{T_d s + 1}{T_f s + 1}, \quad (2.116)$$

so that, by selecting $T_d = T$ (namely, by applying a pole-zero cancellation), the previous case is obtained, where the time constant of the open-loop system is given by T_f .

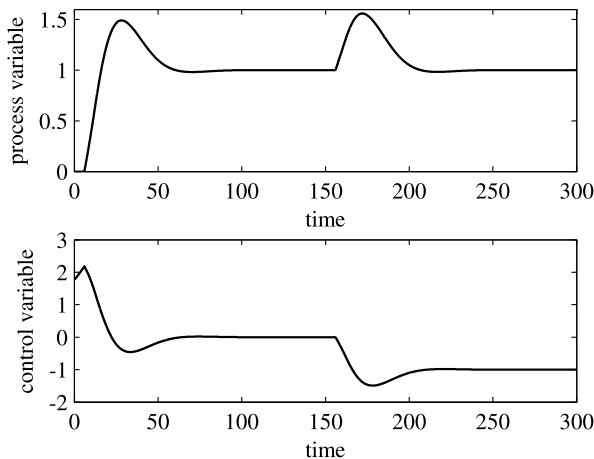


Fig. 2.22 Results obtained with the direct synthesis-based design method based on maximum peak-resonance specification

A particular interesting case is that given by IPDT processes, where $T = 0$. The tuning rules (2.113)–(2.115) are simplified significantly, and they can be related directly (possibly in an automatic tuning context) to the ultimate gain K_u and ultimate frequency P_u of the process as [102]

$$K_p = 0.34K_u, \quad (2.117)$$

$$T_i = 1.04P_u. \quad (2.118)$$

The same process (2.58) is employed as an illustrative example. By applying the proposed method, a PI controller with $K_p = 1.75$ and $T_i = 25$ ($\omega_{\max} = 0.082$) is determined. The resulting set-point and load disturbance unit step responses are plotted in Figure 2.22, while the Nichols chart is shown in Figure 2.21. Obviously, the overshoot in the set-point step response can be reduced by employing a set-point weight.

2.3.3.2 Based on the Minimisation of the Maximum Resonance Peak Value

An approach similar to that of Section 2.3.3.1 has been (previously) proposed in [122]. The approach starts by considering the fact that decreasing the integral time constant in a PI controller for an IPDT process implies that the stability margin of the system decreases as well. Thus, there is a minimum value of the integral time constant below which a reasonable damping cannot be achieved for a given system. The design method consists therefore in specifying the maximum resonance peak value and then in determining the smallest integral time constant for which this value is attained. If an IPDT process with a PI controller is considered, the system

of equations (2.109)–(2.110) can be solved analytically without approximating the arctan function with expression (2.112). Thus,

$$\omega_{\max} = \frac{1}{T_i} \left[\frac{T_i - L}{L} \right]^{\frac{1}{2}}, \quad (2.119)$$

and, as a consequence,

$$\arg L(j\omega_{\max}) = -\pi - \frac{L}{T_i} \left(\frac{T_i}{L} - 1 \right)^{\frac{1}{2}} + \arctan \left(\frac{T_i}{L} - 1 \right)^{\frac{1}{2}}. \quad (2.120)$$

In [122] it is suggested to select $M_r = 2$ dB, which corresponds to $\phi_{\max} = -2.23$ rad. With this value, by solving $\arg L(j\omega_{\max}) = \phi_{\max}$, it results

$$\frac{T_i}{L} = 8.75, \quad (2.121)$$

from which the value of the integral time constant T_i is determined. The proportional gain can be selected at this point in order for the resulting resonance peak value to be at a minimum. By applying this procedure to several numerical cases it has been found that the value of K_p that provides this result can be expressed as a function of the dead time and of the gain of the process:

$$K_p = \frac{0.487}{KL}. \quad (2.122)$$

If process (2.58) is considered, by applying the tuning rules (2.121)–(2.122), we have $T_i = 52.5$ and $K_p = 1.6$. The resulting set-point and load disturbance unit step responses are plotted in Figure 2.23.

2.3.3.3 Based on the Specification of the Desired Control Signal

An original approach, based on the specification of the desired control signal, has been proposed in [139]. Basically, for an IPDT process (2.14), the technique consists in selecting the transfer function between the set-point r and the control variable u as

$$Q(s) := \frac{U(s)}{R(s)} = \frac{s}{K} \frac{(2\xi\tau + L)s + 1}{\tau^2 s^2 + 2\xi\tau s + 1}, \quad (2.123)$$

where the time constant τ is chosen as

$$\tau = \alpha L. \quad (2.124)$$

It has to be stressed at this point that if a step signal of amplitude A_r is applied to the set-point, transfer function (2.123) implies that the desired control signal has an

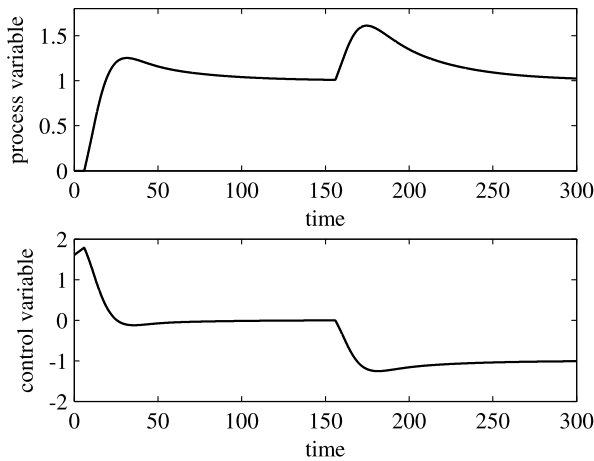


Fig. 2.23 Results obtained with the method based on the minimisation of the maximum resonance peak value

initial change of $(2\alpha\xi + 1)A_r/(\alpha^2KL)$ and then decays exponentially to zero following a second-order system response with normalised time constant α and damping factor ξ . Given a desired damping factor (which is suggested to be either 0.707 or 1), this fact can be obviously exploited for the selection of the design parameter α in order to address the actuator constraints.

Given $Q(s)$, the desired closed-loop transfer function between the set-point r and the output y becomes $H(s) := Q(s)P(s)$, and the corresponding desired open-loop transfer function becomes

$$W(s) = \frac{H(s)}{1 - H(s)} = \frac{(2\alpha\xi + 1)Ls + 1}{\alpha^2L^2s^2 + 2\alpha\xi Ls + 1 - [(2\alpha\xi + 1)Ls + 1]e^{-Ls}} e^{-Ls}. \quad (2.125)$$

By considering now the PID controller transfer function (2.2), which can be rewritten as

$$C(s) = \frac{c_2s^2 + c_1s + c_0}{s}, \quad (2.126)$$

where

$$K_p = c_1, \quad T_i = c_1/c_0, \quad T_d = c_2/c_1, \quad (2.127)$$

the actual open-loop transfer function is given by

$$C(s)P(s) = \frac{c_2s^2 + c_1s + c_0}{s} \frac{K}{s} e^{-Ls}. \quad (2.128)$$

With the aim of matching $G(s)$ with the actual open-loop transfer function (2.128), the following transfer function can be defined ($s = j\omega$):

$$M(j\omega) = \frac{j\omega H(j\omega)}{P(j\omega)}. \quad (2.129)$$

This implies that the frequency domain error between $L(j\omega)$ and the actual open-loop transfer function is zero if

$$M(j\omega) = c_2(j\omega)^2 + c_1(j\omega) + c_0. \quad (2.130)$$

If two straight lines are employed to fit the real part $M_R(j\omega)$ of $M(j\omega)$ against ω^2 and the imaginary part $M_I(j\omega)$ of $M(j\omega)$ against ω through two frequencies ω_1 and ω_2 , then the coefficients c_0 , c_1 , and c_2 can be determined analytically (note that, once the parameters α and ξ are selected, Expression (2.129) is known). The two frequencies can be conveniently selected as $\omega_1 = 2\pi/T_s$ and $\omega_2 = 2\omega_1$, where T_s is the desired closed-loop settling time, chosen as $(6\alpha + 1)L$ [138]. The solution is

$$c_0 = \frac{M_R(\omega_1) - M_R(\omega_2)}{3} + M_R(\omega_1), \quad (2.131)$$

$$c_1 = \frac{M_I(\omega_1)}{\omega_1}, \quad (2.132)$$

$$c_2 = \frac{M_R(\omega_1) - M_R(\omega_2)}{3\omega_1^2}, \quad (2.133)$$

from which the PID parameters can be easily derived from (2.127). At this point, it is worth considering the scaled Laplace transform $\hat{s} = sL$ (which naturally leads to a scaling in the time domain with a normalised time variable $\hat{t} = t/L$) and normalised frequencies $\hat{\omega}_1 = \omega_1 L$ and $\hat{\omega}_2 = 2\hat{\omega}_1$. The corresponding transfer function $M(j\hat{\omega})$ is therefore independent of the process parameters, and therefore the (scaled) PID parameters depend only on ξ and α . By considering the selected values of $\xi = 0.707$ and $\xi = 1$ and by interpolating the results for different values of α , the following tuning rules can be derived (the PID parameters are then conveniently rescaled):

$\xi = 0.707$:

$$K_p = \frac{1}{KL} \frac{1}{0.7138\alpha + 0.3904}, \quad (2.134)$$

$$T_i = L(1.4020\alpha + 1.2076), \quad (2.135)$$

$$T_d = \frac{1}{KL} \frac{1}{1.4167\alpha + 1.6999}; \quad (2.136)$$

$\xi = 1$:

$$K_p = \frac{1}{KL} \frac{1}{0.5080\alpha + 0.6208}, \quad (2.137)$$

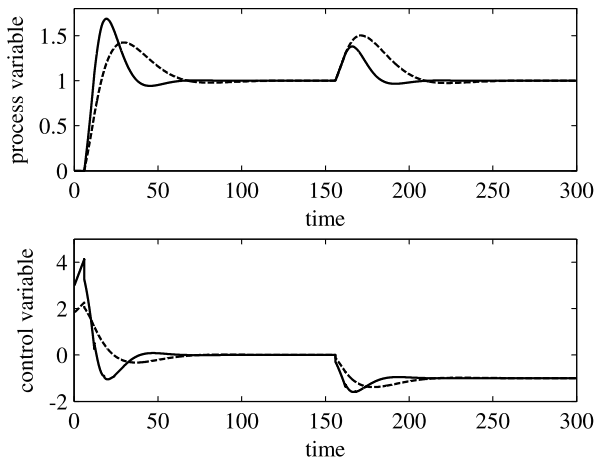


Fig. 2.24 Results obtained with the method based on the specification of the desired control signal (tuning rules (2.134)–(2.136)). *Solid line: $\alpha = 1$. Dashed line: $\alpha = 2$*

$$T_i = L(1.9885\alpha + 1.2235), \quad (2.138)$$

$$T_d = \frac{1}{KL} \frac{1}{1.0043\alpha + 1.8194}. \quad (2.139)$$

If a PI controller has to be employed, it is sufficient to substitute $T_d = 0$ in the above tuning rules.

The same process (2.58) is considered as an illustrative example. By applying the tuning rules (2.134)–(2.136) with $\alpha = 1$, the parameters $K_p = 2.98$, $T_i = 15.66$, and $T_d = 1.93$ are obtained, while with $\alpha = 2$, we obtain $K_p = 1.81$, $T_i = 24.07$, and $T_d = 1.32$. The results related to the set-point and load disturbance step response are shown in Figure 2.24. Conversely, if the tuning rules (2.137)–(2.139) are considered, we obtain $K_p = 2.92$, $T_i = 19.27$, and $T_d = 2.12$ for $\alpha = 1$ and $K_p = 2.01$, $T_i = 31.20$, and $T_d = 1.57$ for $\alpha = 2$. The corresponding results are shown in Figure 2.25. It can be seen that the parameter α can handle effectively the trade-off between aggressiveness and control effort.

2.3.4 Optimisation-based Methods

Tuning rules can be also obtained by minimising a suitable objective function. Methods developed in this context are explained hereafter.

2.3.4.1 Minimisation of the Integral Criteria

Significant attention has been paid by researchers in order to find the tuning of a PID controller that minimises integral performance criteria. This is, in fact, a way to

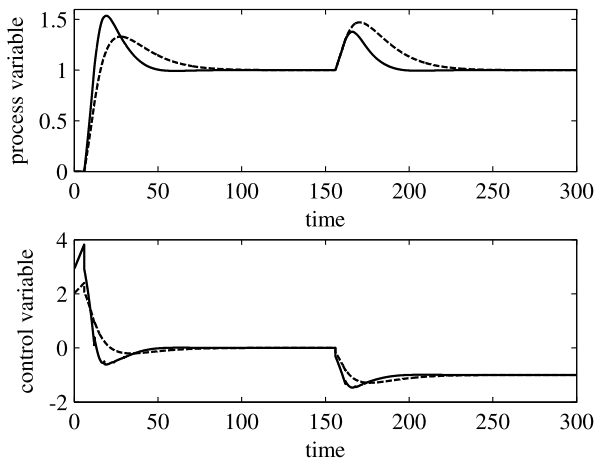


Fig. 2.25 Results obtained with the method based on the specification of the desired control signal (tuning rules (2.137)–(2.139)). *Solid line:* $\alpha = 1$. *Dashed line:* $\alpha = 2$

consider, at the same time, different control specifications, such as a small overshoot and a short settling time. In general, time-moment weighted integral performance indexes are considered. They are defined as

$$J_n(\theta) = \int_0^\infty t^n [e(t; \theta)]^2 dt, \quad n = 0, 1, 2, \quad (2.140)$$

where $\theta = [K_p, T_i, T_d]$ is the vector of (PID) parameters to be selected to minimise (2.140), and $e(t)$ is the system error. Note that $J_0(\theta)$ is denoted as the ISE (Integrated Square Error) criterion, while $J_1(\theta)$ and $J_2(\theta)$ are known respectively as the ITSE and ISTE criteria. A methodology for the determination of tuning formulae which relate the ideal PID coefficients (see (2.2)) to the process parameters K and L (see (2.14)) in order to minimise the objective functions (2.140) has been proposed in [128]. To this purpose, genetic algorithms [74], which are known to provide a global optimum of a problem in a stochastic framework, have been employed. Specifically, many simulations have been performed for different values of the parameter L (obviously, a different value of K results in a simple scaling of the proportional gain) and for different optimisation problems, *i.e.*, considering step changes both in the set-point and in the load disturbance and minimising the three adopted integral criteria (2.140). The optimal PID coefficients found by the genetic algorithms [74] in the different cases have then been analytically interpolated in order to derive suitable tuning rules. These are reported in Table 2.4 for the optimal set-point response and in Table 2.5 for the optimal load disturbance rejection. The symbol ‘–’ which appears in Table 2.4 means that no integral action is required for that case, which is intuitive since the presence of an integrator in the plant assures by itself a zero steady-state error for set-point step changes and adding another integrator in the open-loop transfer function makes the achievement of an acceptable robustness more difficult. From these results it appears that increasing the value of

Table 2.4 PID tuning rules for optimal set-point response

	ISE	ITSE	ISTE
K_p	$\frac{1.03}{KL}$	$\frac{0.96}{KL}$	$\frac{0.90}{KL}$
T_i	—	—	—
T_d	$0.49L$	$0.45L$	$0.45L$

Table 2.5 PID tuning rules for optimal load disturbance response

	ISE	ITSE	ISTE
K_p	$\frac{1.37}{KL}$	$\frac{1.36}{KL}$	$\frac{1.34}{KL}$
T_i	$1.49L$	$1.66L$	$1.83L$
T_d	$0.59L$	$0.53L$	$0.49L$

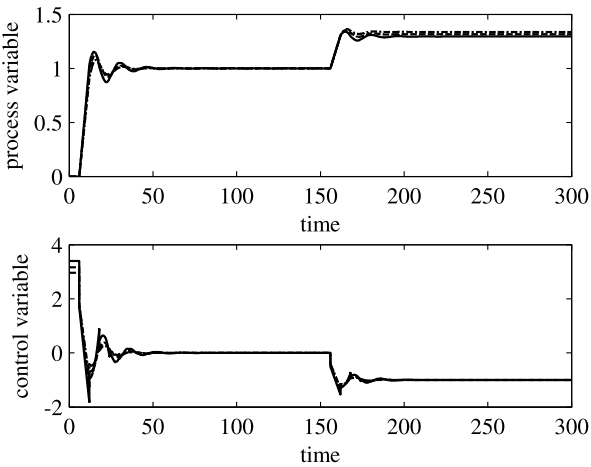


Fig. 2.26 Results obtained with the method based on the optimisation of integral performance indexes for set-point following task. *Solid line:* ISE. *Dashed line:* ITSE. *Dash-dot line:* ISTE

n from 0 to 2 in the performance index (2.140) implies that the PID gains have to be decreased.

As an illustrative example, if the set-point following task for process (2.58) is considered, by applying the tuning rule of Table 2.5, $K_p = 3.39$ and $T_d = 2.94$ are obtained for the ISE performance index, $K_p = 3.16$ and $T_d = 2.70$ are obtained for the ITSE performance index, and $K_p = 2.96$ and $T_d = 2.94$ are obtained for the ISTE performance index. The results related to both the set-point following and load disturbance rejection task are shown in Figure 2.26 (unit step signals are applied in both cases). It appears that, as expected, a steady-state error emerges in the presence of a constant load disturbance because there is no integral action in the controller. Conversely, if the load disturbance task is considered, by applying the

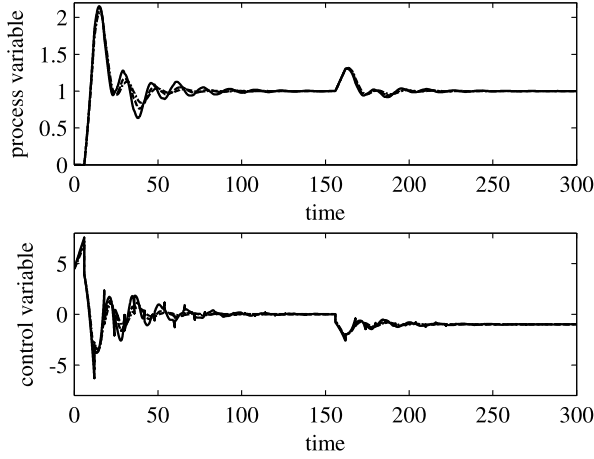


Fig. 2.27 Results obtained with the method based on the optimisation of integral performance indexes for load disturbance rejection task. *Solid line*: ISE. *Dashed line*: ITSE. *Dash-dot line*: ISTE

tuning rule of Table 2.5, $K_p = 4.51$, $T_i = 8.94$, and $T_d = 3.54$ are obtained for the ISE performance index, $K_p = 4.48$, $T_i = 9.96$, and $T_d = 3.18$ are obtained for the ITSE performance index, and $K_p = 4.41$, $T_i = 10.98$, and $T_d = 2.94$ are obtained for the ISTE performance index. The results again relating to both the set-point following and load disturbance rejection tasks are shown in Figure 2.27. As expected, the controller designed for the load disturbance rejection is more aggressive than the controller designed for the set-point following task.

2.3.4.2 Minimisation of an H_∞ Performance Index

A tuning methodology based on the optimisation of an H_∞ criterion has been proposed in [154]. By considering the Internal Model Control scheme of Figure 2.16 and the associated standard unity-feedback control scheme of Figure 2.1 where $C(s) = Q(s)/(1 - P(s)Q(s))$ (see also Figure 2.17), when perfect modelling is assumed, the sensitivity transfer function is

$$S(s) = \frac{1}{1 + C(s)P(s)} = 1 - P(s)Q(s), \quad (2.141)$$

and the complementary sensitivity transfer function is

$$H(s) = \frac{C(s)P(s)}{1 + C(s)P(s)} = P(s)Q(s). \quad (2.142)$$

The transfer function matrix $M(s)$ from the reference input r and the load disturbance input d to y and u is therefore

$$M(s) = \begin{bmatrix} H(s) & P(s)S(s) \\ Q(s) & -H(s) \end{bmatrix}. \quad (2.143)$$

The closed-loop system is internally stable if all the transfer functions in $M(s)$ are stable, which implies that $Q(s)$ is stable and satisfies the following constraints:

$$\lim_{s \rightarrow 0} S(s) = \lim_{s \rightarrow 0} [1 - P(s)Q(s)] = 0, \quad (2.144)$$

$$\lim_{s \rightarrow 0} \frac{d}{ds} S(s) = \lim_{s \rightarrow 0} \frac{d}{ds} [1 - P(s)Q(s)] = 0. \quad (2.145)$$

Then, a SOIPDT process (2.25), where the dead time is approximated by a first-order Taylor series, is considered:

$$P(s) = \frac{K(1 - Ls)}{s(Ts + 1)}. \quad (2.146)$$

The optimal performance criterion to be minimised by the control system is selected as

$$\| \Gamma(s)S(s) \|_{\infty}, \quad (2.147)$$

where $\Gamma(s)$ is a weighting function selected as

$$\Gamma(s) = \frac{1}{s}, \quad (2.148)$$

which implies that the closed-loop system input is a step signal.

If $\tilde{Q}(s) = Q(s)$ (namely, the filter $F(s)$ is neglected), minimising (2.147) yields

$$\Gamma(s)(1 - P(s)\tilde{Q}(s)) = L, \quad (2.149)$$

and therefore the optimal $\tilde{Q}(s)$ is determined as

$$\tilde{Q}(s) = \frac{s(Ts + 1)}{K}. \quad (2.150)$$

It appears that, in order to make $Q(s)$ proper, however, a filter $F(s)$ has to be employed.

If $T = 0$ (namely, an IPDT process is considered), it can be verified that a first-order filter does not satisfy the asymptotic tracking requirement. Thus, the filter is selected as the second-order transfer function

$$F(s) = \frac{as + 1}{(\lambda s + 1)^2}, \quad (2.151)$$

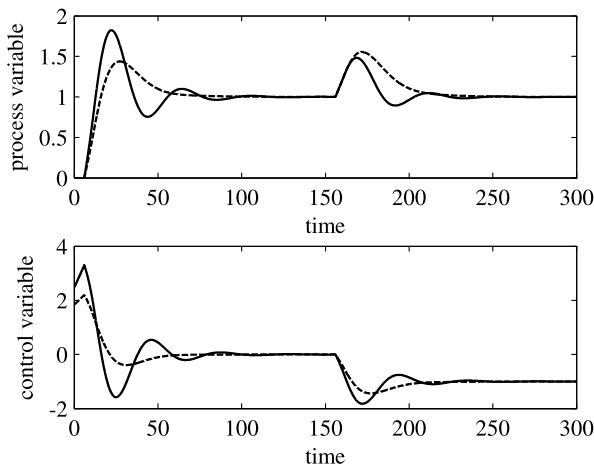


Fig. 2.28 Results obtained with method based on the minimisation of an H_∞ performance index. *Solid line:* $\lambda = 6$. *Dashed line:* $\lambda = 12$

where, according to (2.145), $a = 2\lambda + L$. Thus, by considering $Q(s) = \tilde{Q}(s)F(s)$ and $C(s) = Q(s)/(1 - P(s)Q(s))$ a PI controller is obtained with

$$K_p = \frac{2\lambda + L}{K(\lambda + L)^2}, \quad (2.152)$$

$$T_i = 2\lambda + L. \quad (2.153)$$

By applying the same reasoning, if a SOIPDT model is considered, the filter can be selected as

$$F(s) = \frac{as + 1}{(\lambda s + 1)^3}, \quad (2.154)$$

where $a = 3\lambda + L$ is determined from (2.145). The resulting controller is an output-filtered PID controller (2.4) with

$$K_p = \frac{3\lambda + L + T}{K(3\lambda^2 + 3\lambda L + L^2)}, \quad (2.155)$$

$$T_i = 3\lambda + L + T, \quad (2.156)$$

$$T_d = \frac{(3\lambda + L)T}{3\lambda + L + T}, \quad (2.157)$$

$$T_f = \frac{\lambda^3}{3\lambda^2 + 3\lambda L + L^2}. \quad (2.158)$$

As in IMC, the user-chosen parameter λ can handle the trade-off between aggressiveness and robustness. As an example, if the process (2.58) is considered, the PI controller with $K_p = 2.47$ and $T_i = 18$ is obtained from the tuning rules (2.152)–(2.153) by selecting $\lambda = L = 6$, while for $\lambda = 2L = 12$, the parameters $K_p = 1.83$

and $T_i = 30$ are obtained. Results related to the set-point and load disturbance step response are shown in Figure 2.28.

2.4 Conclusions

In this chapter, the use of PID controllers for the control of integral processes has been addressed. After an introduction on PID controllers, it has been shown that this kind of controllers can be employed effectively for both the set-point following and load disturbance rejection tasks, especially if the control requirements are not too tight. Both open-loop and closed-loop techniques for the estimation of the process parameters have been described. Then, starting from the model obtained, different approaches have been presented for the tuning of the PID parameters with the aim of showing that the tuning problem can be tackled from different viewpoints, each with specific features.



<http://www.springer.com/978-0-85729-069-4>

Control of Integral Processes with Dead Time

Visioli, A.; Zhong, Q.

2011, XXV, 250 p., Hardcover

ISBN: 978-0-85729-069-4